

# VoMIR: OVER 300 VOLCANOES MONITORED IN NEAR REAL-TIME BY AATSR

Colin, O. , Rubio, M. , Landart, P. and Mathot, E.

European Space Agency – ESRIN, via Galileo Galilei 00044 Frascati, Italy  
{Olivier.Colin, Miguel.Angel.Rubio.Escudero, Paula.Landart, Emmanuel.Mathot}@esa.int

## ABSTRACT

The Along Track Scanning Radiometer (ATSR-2) on board the ERS-2 satellite has demonstrated to be very valuable to global volcanological research and surveillance applications [Wooster and Rothery, 2000]. Early 2000, a prototype service was developed and put into operations at ESA to monitor in near real-time the thermal activity of more than 100 volcanoes worldwide. The prototype based on a theoretical orbiting model was unfortunately discontinued early 2001 after the failure of the digital earth sensor of the spacecraft subsequently operated under the gyro-less attitude control mode.

Using AATSR (Advanced ATSR) flying on board the Envisat spacecraft, this near-real-time service called Volcanoes Monitoring by Infra-Red (VoMIR) was revived with enlarged coverage of 361 volcanoes, improved algorithm and appealing end-user tools for data display.

Since early April 2007, the VoMIR products can be visualised and downloaded freely from Internet at

<http://earth.esa.int/vomir>

This paper summarises the rationale of VoMIR, algorithm and output.

## 1. VOMIR SERVICE OUTLINE DESCRIPTION

Using AATSR data, the VoMIR service aims at providing a global-scale thermal mapping of volcanic activity, specifically targeting the real-time publishing of geothermal instant observations over every volcano, together with long-term trends pertinent to monitoring the activity along time. The VoMIR products are primarily intended to serve science research bodies involved in volcanology, global geothermal studies, geology, etc.

VoMIR processing is performed on ESA's multipurpose Grid Processing-on-Demand Environment (G-POD). Soon after data acquisition, results are made publicly available on the web.

The user can select the volcano or volcanoes of interest from a world map or a list of all the volcanoes available, select the time interval to retrieve and visualise or download all the records available from the server through the service web-pages [Figure 1].

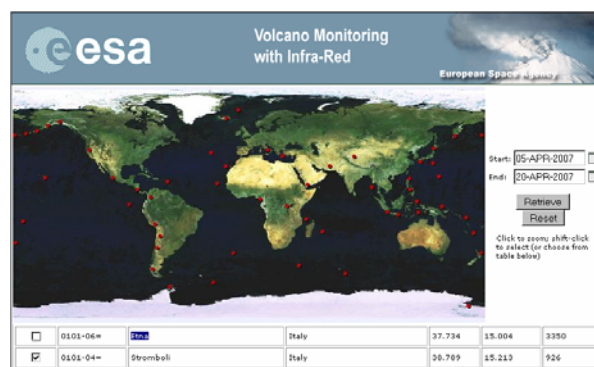


Figure 1 – VoMIR Query WebPage

The whole ENVISAT mission from year 2003 onwards is available for retrieval and is updated with every new ENVISAT overpasses over the volcanoes.

## 2. RATIONALE

The Global Volcanism Program [GVP] makes the inventory of nearly 3000 active volcanoes worldwide [Figure 2], of which more than 550 are categorised with a dated record of a “recent” eruption, and about 500 within the last 200 years. This large database maintains the long-term eruptive history of each volcano and is today populated by heterogeneous sources mainly compiling in-situ observations provided by local surveillance institutions and complemented sporadically by space-borne observations.

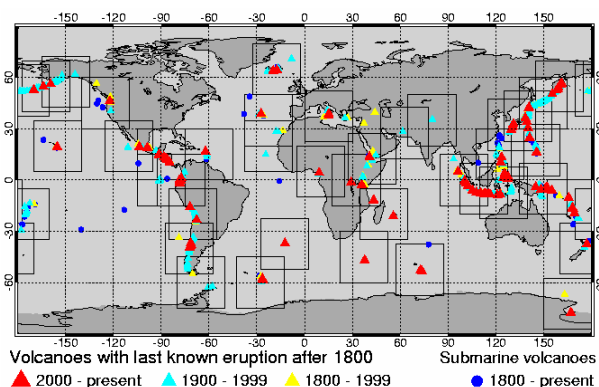


Figure 2 - Worldwide Volcanoes and Timeframes of Eruptive Activity - courtesy of the Volcanic SO2 Service home page [TEMIS/VSO2S]

Although wide-ranging research achievements on the relevance of space-borne remote sensing techniques to volcano monitoring has matured in the science domain since the 1960s, little “global” data from earth-observation satellites is readily available operationally to support its potential users.

*Nonetheless operational services worth mentioning here are: the ATSR World Fire Atlas product published by ESA [IONIA/WFA] and operational since 1995 which classifies hot spots worldwide using the ATSR instrument series; Similarly, the global thermal alert system [MODVOLC] hosted by the university of Hawaii publishes on-line and in near-real-time the Normalised Thermal Index (NTI) based on MODIS data; Other than thermal imagery, NASA and the University of Maryland jointly publish in near-real time ozone and ash aerosol maps over erupting volcanoes [TOMS]; Similarly, KNMI should soon host operationally the global Volcanic SO<sub>2</sub> service based on SCIAMACHY data [TEMIS/VSO2S].*

The ATSR series of space borne instrumentation (ERS-1, ERS-2, Envisat) is highlighted as ideal for continuous thermal mapping of global-scale volcanic activity [Wooster et al., 2000]. Major assets of the instrument in this respect are:

- Its contemporaneous thermal imaging capability in four complementary infrared bands: two thermal infrared (TIR) channels (11µm and 12µm), one medium infrared (MIR) channel (3.7µm) and more noteworthy one short wave infrared (SWIR) channel centred at 1.6µm particularly suited to measuring the potentially high temperature range of volcanic sources.
- The relatively high temporal resolution of the dataset it can generate over any site on earth (every 3 days in average) by day and night.
- Its relatively high spatial resolution (1km) as compared other thermal imaging devices e.g. mounted on board geo-stationary satellites (e.g. GOES).
- The dual viewing capability of the instrument (Nadir and Forward views) providing two observation angles with two independent observation paths through the atmosphere to the target

### 3. ALGORITHM

The VoMIR enhanced algorithm is building upon the initial work of [Arnaud et al], and is mostly inspired from existing outstanding literature on the subject and

more specifically on the work of M.J.Wooster and D.A.Rothery ([Wooster and Rothery 1997], [Wooster and Rothery, 2000], [Rothery et al., 2001]).

The AATSR level-1B GBT product is used in input and only the night time observations over the volcanoes are considered.

The algorithm applies two separate methods (in some cases concurrent) to volcanic thermal activity detection. Both methods are summarised hereafter.

#### 3.1. Primary detection method (1.6µm Analysis)

The primary approach is considering above all the 1.6µm channel response, applying for hot spot classification a fixed threshold to the measured radiance. The simple threshold approach is considered adequate for unambiguously detecting the presence of volcanic related thermal sources within the volcano mask. In effect, as it can be understood from the Planck distribution of Figure 3, this wavelength band will detect thermal radiations emitted by temperature sources ranging above 200°C. As such, it will not be spoiled by thermal contributions of emitters at background temperatures. The threshold applied on the radiance is however required to unambiguously avoid channel noise.

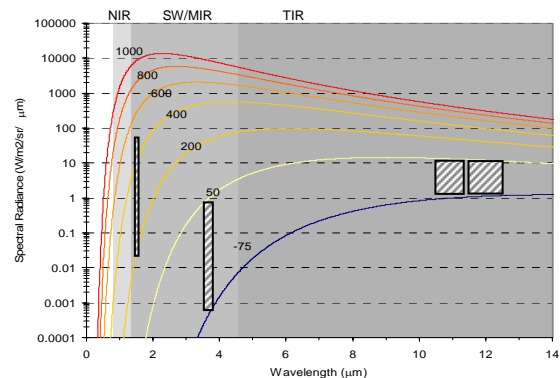


**Figure 3 - Blackbody spectral radiances according to Planck's Radiation Law for temperatures ranging between -75°C and 1000°C. The hashed rectangles represent each of the AATSR channels centred at 1.6µm (SWIR), 3.7 (MIR), 11µm and 12µm (TIR). The box width represents the channel bandwidth of each sensor.**

Moreover, although the volcanic thermal sources may range above 500°C up to 1000°C, the overall short wave contribution of very hot (>500°C) to magmatic surfaces (>950°C) are never expected to saturate the 1.6µm channel receiver since they are most frequently spanning only a small fraction of the one square-meter footprint of the AATSR pixel, and as such will be spatially averaged with substantially lower temperature contributors in the 1m<sup>2</sup> pixel area.

### 3.2. Secondary detection method (3.7µm Thermal Anomaly Analysis)

The secondary approach is complementary to the primary one and intends as primary goal to detect the thermal emissions from hot sources of relatively lower thermal magnitude, which would be invisible in the 1.6µm channel response or fall under the noise threshold.

For this, it uses as primary input the radiance emitted in the MIR channel receiver (3.7µm). As explained by [Wooster and Rothery, 2000] and as indicated on Figure 3, for temperatures below ~950°C, more energy is emitted at 3.7µm than at 1.6µm, and significant emittance at 1.6µm ceases at around 400°C but continues to much lower temperatures at 3.7µm.

However, this advantageous trade-off brought in by the 3.7µm channel sensitivity makes this wavelength more inclined to saturation, and to capturing spurious energy complements emitted by non-volcanic sources, such as the one of the background.

The case of saturation is not considered in this approach as it is expected the primary method would in any case respond positively to the hot spot detection in such cases.

To minimise the contribution of the background temperature to the energy measured at 3.7µm, a method inspired from [Kaneko et al., 2002] is applied using the brightness temperature reflected at 11µm. The principle resides in the computation of the thermal anomaly (THA) 3.7µm radiance corresponding to the resulting energy that would be emitted at 3.7µm by volcanic hot spots if no other background temperature emitter were present within the pixel area.

In effect, as explained by [M.J.Wooster, 1997] and directly derived from the Planck formula, a hot source ( $T > 300^\circ\text{C}$ ) will radiate at 11µm according to approximately the square of the temperature whilst the 3.7µm energy will be roughly proportional to  $T^4$ . This fact allows small hot source contributors to be clearly visible at 3.7µm when their contribution at 11µm is minimised.

In consequence, the resulting brightness temperature measured at 11µm will be in such cases lower than the one at 3.7µm as simulated by [M.J.Wooster, 2000] and illustrated on Figure 4.

It is further expected that in case the full 1m<sup>2</sup> AATSR pixel area were uniformly hot, both channels would relate an identical temperature for the target. Thus the THA detection is expected to detect hot sources of sub-pixel size.

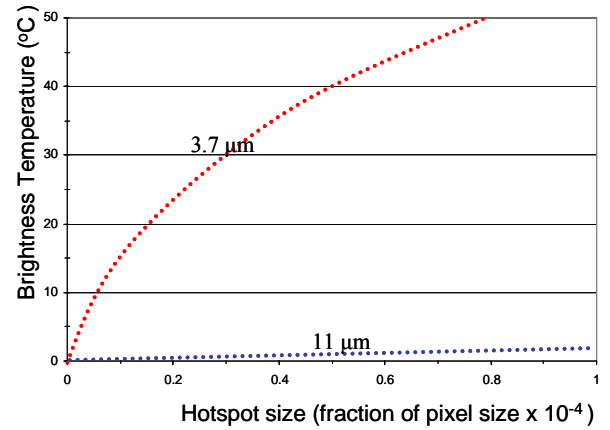


Figure 4 - Model of a dual thermal component response in the 3.7µm and 11µm wavelengths - The modelled pixel has a background temperature of 0°C and contains a sub-pixel-sized hot spot at 500°C. The whole 1m<sup>2</sup> pixel brightness temperature is plotted for situations where the hotspot varies from nothing to 1/1000th of the pixel area. As the hotspot size increases, the 3.7µm brightness temperature increases sharply whilst the 11µm brightness temperature increases only slowly

The major enhancement provided to the VoMIR method as compared to the one described in [T.Kaneko et al, 2002] resides in the approach followed to compute the brightness temperature difference ( $BT_{3.7\mu\text{m}} - BT_{11\mu\text{m}}$ ) of the background, used subsequently to unambiguously avoid the THA positive detections potentially inferred by non-volcanic sources (e.g. hot clouds).

This filtering step is of primary importance to the hot spot detection since, as it was confirmed by [R.Wright et al., 2002], hot clouds can share similar behaviour as active lava as regarding the BT difference figure, which led them to the definition of MODIS NTI (Normalised Thermal Index) to improve the hot-spot classification.

In the case of AATSR, it was observed that hot cloud pixels might exhibit a ( $BT_{3.7\mu\text{m}} - BT_{11\mu\text{m}}$ ) difference as high as 20°C, which would by strictly applying the method of Kaneko lead to wrong detection.

This indeed motivated the enhancement provided in the VoMIR method, by using the radiance at 1.6µm as explained hereafter:

A statistic is made for all pixels surrounding the pixel under study (within a radius of 7.5 km) of the ( $BT_{3.7\mu\text{m}} - BT_{11\mu\text{m}}$ ) difference considering only positive values and pixels that do not exhibit a significant signal in the 1.6µm channel. Using a pixel mask based on the 1.6µm signal ensures the high contributors (i.e. potential hot spots) will not contribute to it.

Based on this statistic, the THA detection will consider only the pixels not classified as cloudy and such that:

$$(BT_{3.7\mu\text{m}} - BT_{11\mu\text{m}}) > M_{\text{bknd}} + 3 \sigma_{\text{bknd}}$$

Where  $M_{bknd}$  and  $\sigma_{bknd}$  are respectively the Mean and Standard deviation resulting from the background classification statistic.

For those pixels, the THA 3.7 $\mu$ m radiance (or radiance anomaly) is then computed by subtracting the background temperature component to the 3.7 $\mu$ m-received energy.

Finally, detection will respond positively (i.e. containing volcanic hot sources) for all pixels resulting in a radiance anomaly above a given threshold.

This method provides to date a-priori satisfactory results in a variety of heterogeneous volcano sites, ranging between cold high-relief areas or seashore tropical areas. Nevertheless, it was observed the current algorithm tends to sometimes wrongly detect hot pixels in the crater, in particular at Mount Etna during the winter season, the crater being relatively hotter than its surroundings generally covered with snow.

### 3.3. Cloud Detection

Cloud clearing is essential to VoMIR processing as clouds may mask partially or entirely the AATSR ground pixels and in consequence infer on the hotspot detection. In particular, the algorithm will only conclude on a volcano inactivity when no pixel within the studied area is classified as cloudy. In addition, quality flags are provided together with each VoMIR observations qualifying the cloud coverage as well as the percentage of hotspots detected in the immediate neighbourhood of clouds.

VoMIR uses the cloud classification stamped in the products by the AATSR Level-1B processor. Cloud clearing applied to land surfaces and night-time observations is a complex task, and the Level-1B algorithms appear to often conclude inaccurately for cloudiness in particular over high-latitude areas (e.g. polar volcanoes) or high-altitude areas (e.g. Andes) where the ground temperature is low.

At this stage, the VoMIR processor uses only a subset of the Level-1B processor cloud tests to identify a pixel as cloudy: The 11/3.7 micron fog/low-stratus test specific to night-time measurements and the 11/12 micron thin cirrus test. A more in-depth study of specific cloud clearing algorithms to be applied over volcanoes shall at term complement this lack.

## 4. ALGORITHM VERIFICATION AND TUNING ON ESA'S GRID PROCESSING-ON-DEMAND

The VoMIR processor has been integrated on the Grid Processing-on-Demand environment [G-POD] deployed at ESRIN.

This infrastructure, building upon Grid computing technology, provides an environment where application

services can be seamlessly plugged into. Coupled with the high-performance data processing capability of the ESA local Grid (95 x dual-CPU high performance computing elements), as well as a large distributed data-store holding the EO missions products (>90TB), it provides the necessary flexibility for building an application virtual environment with quick accessibility to the earth observation data, computing resources and results.

In order to ease the prototyping, as well as algorithm tuning and verification activities, the VoMIR processor provides a configuration interface [Figure 5] by which the core of the algorithm can be customised at will through a set of rules. The rules, following a typical computer language syntax are then interpreted at run-time by the processor when the processing jobs are submitted. Figure 5 highlights the rule definition dialog on the job submission page where algorithm customisations are defined.

This functionality has allowed in particular swift customisations to be made between two runs e.g. on the detection thresholds and/or overall algorithm logic of the THA analysis, in turn allowing to easily compare the performance of different versions of the algorithm, and to fine-tune the algorithm parameters experimentally.



Figure 5 – VoMIR prototype job submission page on the G-POD portal during algorithm tuning - The processing can be further customised via the redefinition or customisation of the default VoMIR algorithmic rules and associated parameters.

As importantly, the processing capacity offered by G-POD as well as its privileged access to the Envisat

mission products allows a full year of AATSR level-1B data to be processed over a volcano in about 10 minutes. Such performance is the key enabling factor to the intended fine-tuning, and forthcoming verification and validation activities.

## 5. VOMIR OUTPUT

All VoMIR output products are published on-line and can be visualised or downloaded through the query interface. Figure 6 depicts an example of the result page after a query over Stromboli between June 2006 until May 2007.

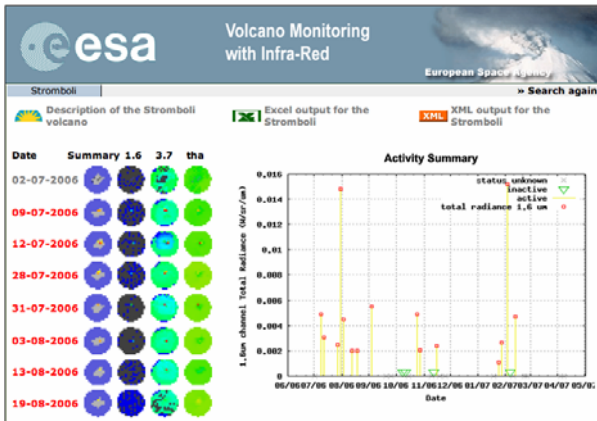


Figure 6 – Example of VoMIR Query Result WebPage

### 5.1. Excel Output

All detailed measurements over the defined period are provided under the form of an Excel spreadsheet per volcano [Figure 7] compiling all measures, statistics, quality indicators and quick look images corresponding to each observation. This output allows in particular other correlations and graphs to be further created using Excel functionality.

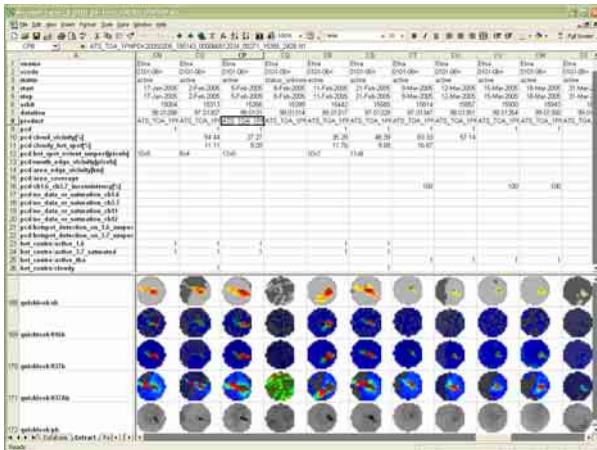


Figure 7 – Example of VoMIR Output Excel Data Sheet

### 5.2. Google Earth Displays

Each VoMIR observation can be additionally displayed in the Google Earth Client (public version). The recent

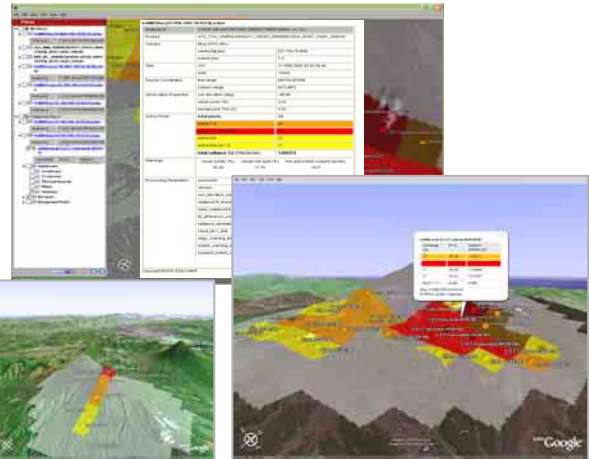
public release of this powerful tool makes it a real asset for displaying and sharing geographical information.

The case of VoMIR output displays is particularly relevant:

- ❑ The summary results can be provided in HTML [Figure 8-a]
- ❑ The generated quick-look images compiled over the volcano mask can be overlaid on top of the background layers and DEM of Google Earth, providing impressive correlated views of the measurements with the terrain [Figure 8-b/c].
- ❑ The detailed AATSR source observations at 1km resolution together with the VoMIR elaborated data over each pixel can be displayed in documented Placemarks overlaid on the map view [Figure 8-c]. This powerful feature allows in particular a close verification of the algorithm logic and dependency vis-à-vis the input data and the algorithm thresholds.

The VoMIR Google Earth views are provided in the standard KML format and don't exceed 50KBytes in average.

a) VoMIR summary over Etna, 11<sup>th</sup> February 2005



b) Fuego, April 2003

c) Etna, 11<sup>th</sup> February 2005

Figure 8 – Examples of VoMIR Google Earth Displays

### 5.3. XML Products

In addition, to allow easier retrieval and post-processing of VoMIR results through automated means, the VoMIR records are provided in raw XML format with all details.

### 5.4. Summary Activity Status Graph

A summary graph per volcano summarises the volcano activity along time [Figure 9]. The plotted quantity is the compound volcanic energy at 1.6μm received by AATSR (expressed in W/sr/μm), obtained by summing up the received radiance of all pixels classified as volcanic hot-spots.

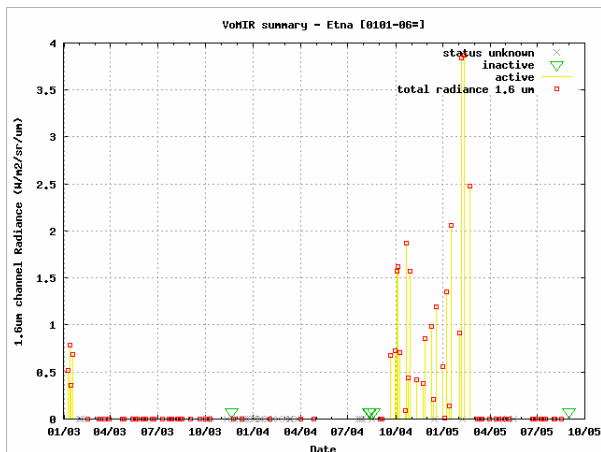


Figure 9 - 1.6µm Total Radiance over Etna from year 2003

In the case of Etna, a peak energy is observed on the 11th February this year (3.8 W/sr/µm) after long eruption that began on the 7th September 2004.

## 6. CONCLUSIONS AND FUTURE PROSPECTS

The VoMIR processor provides encouraging results, the secondary hot spot detection method acting complementarily to the first one in detecting small-sized hot surfaces that remain invisible in at 1.6µm.

Its current implementation on G-POD enables swift experimental fine-tuning to be performed to further improve the algorithm performance. The binding of the VoMIR output with the Google Earth browser substantially empowers the application by providing an integrated environment offering powerful display capabilities and which can easily be shared over the internet in a collaborative process, such as during validation.

Efforts will now be concentrated along two main axes. One will be the exploitation of the ATSR-2 product archive to provide a 12-years long-term record of VoMIR measurements across ERS-2 and Envisat missions. As importantly, the second will aim at translating the VoMIR “remote-sensing” product into more volcanological terms, to support end-users such as civil organisations involved in volcanic and seismic hazards prediction, emergency management, airline safety, etc.

## 7. REFERENCES

### 7.1. Articles

- Arnaud A., Wooster M., Arino A., Bequignon J., Goryl P., 1999. Use of ERS ATSR-2 for Volcanoes Monitoring by InfraRed. IGAARRS 1999 - Hamburg
- Fusco, L., Gonçalves, P., Linford, J., Fulcoli, M., Terracina, A., D'Acunzo, G., 2003. Putting Earth-

Observation Applications on the Grid. ESA Bulletin, No 114, May 2003, pp.86-90

- Harris A.J.L., Murray J.B., Aries S.E., Davies M.A., Flynn L.P., Wooster M.J., Wright R. and Rothery D.A., 2000. Effusion rate trends at Etna and Krafla and their implications for eruptive mechanisms. *Journal of Volcanology and Geothermal Research* 102 (2000) 237–270
- Kaneko T., A. Yasuda A., Ishimaru T., Takagi M., Wooster M.J. and Kagiya T., 2002. Satellite Hot Spot Monitoring of Japanese Volcanoes: A Prototype AVHRR-based System, *Advances in Environmental Monitoring and Modelling*, <http://www.kcl.ac.uk/advances>, Vol. 1 No. 1 (2002) pp.125-133
- Rothery D. A., Coltelli M., Pirie D., Wooster M. J., Wright R., 2001. Documenting surface magmatic activity at Mount Etna using ATSR remote sensing. *Bull Volcanol* (2001) 63:387–397
- Wooster M.J. and Rothery D.A., 2000. A Review of Volcano Surveillance Applications Using the ATSR Instrument Series. In: *Advances in Environmental Monitoring and Modelling*, Vol. 1 No. 1 (2000) pp.3-35
- Wooster M.J. and Rothery D.A., 1997. Thermal monitoring of Lascar Volcano, Chile, using infrared data from the along-track scanning radiometer: a 1992–1995 time series. *Bull Volcanol* (1997) 58 : 566–579
- Wright R., Flynn L.P., Garbeil H., Harris A.J.L. and Pilger E., 2002, Automated volcanic eruption detection using MODIS: Remote Sensing of Environment, v. 82, p. 135-155.

### 7.2. Web Resources

- [GVP] Global Volcanism Program, National Museum of Natural History, Smithsonian Institution <http://www.volcano.si.edu/>
- [IONIA/WFA] ATSR World Fire Atlas, European Space Agency. <http://dup.esrin.esa.int/ionia/wfa/>
- [MODVOLC] Near-real-time thermal monitoring of global hot-spots. Hawai'i Institute of Geophysics and Planetology, University of Hawai'i at Manoa. <http://modis.higp.hawaii.edu/>
- [TOMS] Volcanic Emissions Group, University of Maryland, Baltimore County. <http://toms.umbc.edu/>
- [TEMIS/VSO2S] Volcanic SO2 Service, Koninklijk Nederlands Meteorologisch Instituut (KNMI). <http://www.temis.nl/>
- [G-POD] Grid Processing-on-Demand (ESA). <http://eogrid.esrin.esa.int>

